

Magnetic anisotropy of epitaxial Fe/Pt(001) multilayers

Makoto Sakurai

Advanced Materials Research Laboratory, Tosoh Corporation, Hayakawa 2743-1, Ayase, Kanagawa 252, Japan

(Received 15 December 1993; revised manuscript received 10 March 1994)

The structure of epitaxial Fe/Pt(001) multilayers deposited by *e*-beam evaporation was characterized by a four-circle x-ray diffractometer and the magnetic anisotropy was investigated using a torque magnetometer. For epitaxial Fe/Pt(001) multilayers, a structural transition of the Fe layer is found to occur with increasing Fe layer thickness. The critical thickness is around 8 Å. Magnetic anisotropy and coercive force change with the transition. The out-of-plane volume anisotropy decreases for the Fe layer thickness less than 8 Å. The fourfold in-plane anisotropy is lost for the Fe layer thickness less than 8 Å. For the Fe layer thickness beyond 8 Å, it is found that the in-plane interface anisotropy is negative and that the in-plane volume anisotropy is identical to the magnetocrystalline anisotropy of bulk bcc Fe.

I. INTRODUCTION

Ultrathin magnetic layers and multilayers are subjects of intense current research because of their novel properties and potential device applications. The magnetic anisotropy arising from the interfaces between magnetic and nonmagnetic layers is an important problem in magnetism. Magnetic anisotropy for a multilayer was phenomenologically separated into the interface and volume anisotropies.¹ The volume anisotropy is the sum of magnetostatic, magnetocrystalline, and magnetoelastic anisotropies. On the other hand, the mechanism of the interface anisotropy has not well been understood. There should exist a magnetostatic contribution.² The interface anisotropy is related to the electronic structure and also the stress at the interfaces as are suggested from the following results. The interface anisotropies for Au/Cu/Au/Co (Ref. 3) and Pd/Au/Pd/Co (Ref. 2) multilayers were found to depend strongly on the Au and Pd layer thicknesses. For an ultrathin Co(001) film, the interface anisotropy is very sensitive to the presence of a Cu overlayer.⁴ Photoemission and inverse photoemission experiments show a modification of electronic structure due to the two dimensionality and an enhancement of exchange splitting at the interface.^{5,6} The calculation based on the local-spin-density approximation suggests that the large spin-orbit interaction for a Co/Pd system contributes to the perpendicular magnetic anisotropy.⁷

Single crystalline Fe films have been investigated from structural and magnetic viewpoints. Metastable fcc Fe on Cu(001) has been studied extensively because of both their novel structure⁸ and their unusual magnetic properties.^{9,10} The magnetic anisotropy of Fe(110) on W(110) was investigated by Elmers and Gradmann.¹¹ Epitaxial Fe/Au(001) multilayer shows oscillatory magnetoresistance with varying Au layer thickness.¹² Recently epitaxial Fe/Pt(001) multilayer¹³ and FePt(001) films with perpendicular magnetic anisotropy¹⁴ have been studied.

In this paper, we show by the off-axial x-ray measurements that the Fe layer for an epitaxial Fe/Pt(001) multilayer undergoes a structural transition with increasing Fe layer thickness. We study how magnetic anisotropy and

magnetization change with the transition. These properties were compared with those of Fe/Ag(001) and polycrystalline Fe/Pt multilayers. The lattice mismatch between bulk bcc Fe(001) and fcc Pt(001) is about 3%. On the other hand, the mismatch between bcc Fe(001) and fcc Ag(001) is relatively small. The out-of-plane and in-plane magnetic anisotropies are measured to study the mechanism of anisotropy in more detail.

II. EXPERIMENT

Samples were prepared by *e*-beam evaporation in an ultrahigh-vacuum chamber of a base pressure around 1×10^{-9} Torr. MgO(001) substrates were heated in the chamber at 450°C for 15 min and then a 500-Å Ag(001) buffer layer was deposited at 50°C on a thin Cr (~15 Å) seed layer.¹⁵ The Pt and Fe layers were alternately grown onto the buffer at a rate of 0.2 Å/sec. The number of repetitions was fixed to 15. The Fe/Ag(001) multilayers were produced under a similar condition, and polycrystalline Fe/Pt multilayers were deposited on oxidized Si(111) substrates. Magnetic anisotropy and structure for epitaxial Fe/Pt(001) multilayers were systematically investigated with fixing the Pt layer at 13.5 Å and varying the Fe layer thickness from 3.3 to 33.6 Å. The structure of the multilayer was studied by x-ray-diffraction measurement using a four-circle diffractometer (Huber 420.511)¹⁶ and cross-sectional transmission electron microscopy (TEM). Magnetic anisotropy and magnetization at room temperature were measured by a torque magnetometer and by a vibrating sample magnetometer, respectively.

III. RESULTS AND DISCUSSION

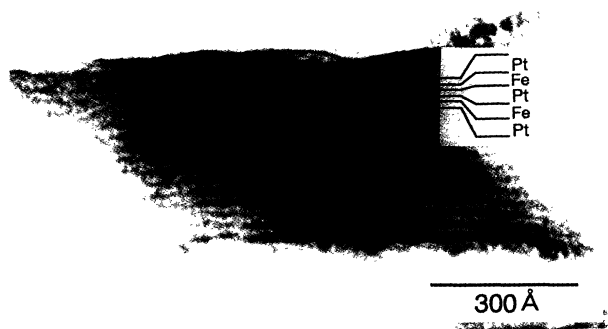
A. Structure

A cross-sectional TEM image of [Fe(8.4 Å)/Pt(13.5 Å)]₁₅ (001) multilayer is shown in Fig. 1(a). The dark bands correspond to Pt layers and the light ones to Fe layers. The figure indicates the establishment of a multilayered structure. Figure 1(b) shows the electron-

diffraction pattern for the cross-sectional specimen with the electron beam along Pt[100]. The spots along the Q_y and Q_z direction suggest in-plane and out-of-plane epitaxial relations, respectively. The spots cannot be separated into those of Fe and Pt because of its short modulation length. Both of the average lattice spacings, $d_{(020)}$ and $d_{(002)}$, are 1.95 Å. It suggests a fcc structure of the superlattice. The satellite peaks along the Q_z direction are due to the modulation of the multilayer. Spots of MgO substrate and Ag buffer layer are not observed, since they are eliminated by standard mechanical thinning and ion milling during sample preparation. A typical x-ray diffraction pattern for a $[\text{Fe}(5 \text{ \AA})/\text{Pt}(13.5 \text{ \AA})]_{15}$ (001) multilayer is shown in Fig. 2. The observed satellite spacing corresponds to the period of the multilayer. The rocking curve widths of the buffer layer and the main peak are 0.64° and 1.2° , respectively.

To study the structure of epitaxial Fe/Pt(001) multilayer in more detail, we measured off-axial x-ray diffraction. Figure 3 shows a reciprocal lattice space of an fcc metal. For the present multilayer, the Q_x and Q_y axes are taken along [200] and [020] directions of the Ag buffer layer

(a)



(b)

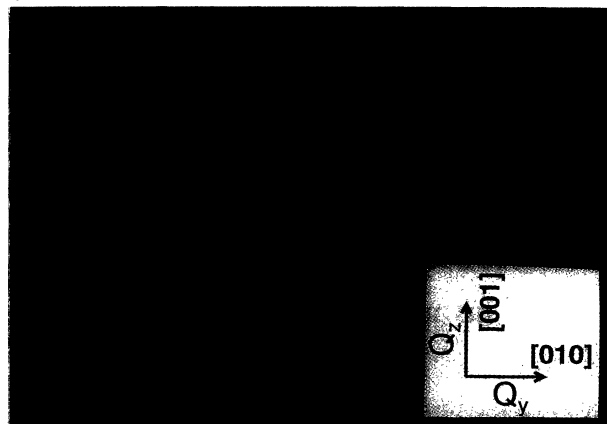


FIG. 1. (a) Cross-sectional TEM image for a $[\text{Fe}(8.4 \text{ \AA})/\text{Pt}(13.5 \text{ \AA})]_{15}$ (001) multilayer. (b) Electron diffraction pattern for the cross sectional specimen, taken with the electron beam along Ag[100]. The satellite peaks along the Q_z direction show the modulation of the multilayer.

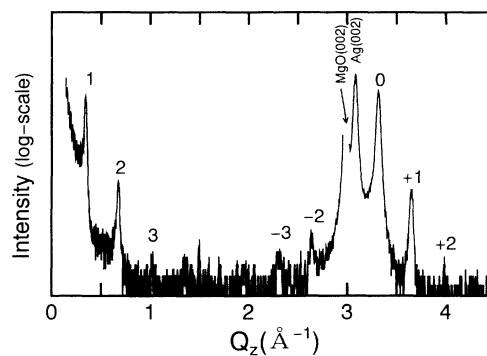


FIG. 2. X-ray diffraction for a $[\text{Fe}(5 \text{ \AA})/\text{Pt}(13.5 \text{ \AA})]_{15}$ (001) multilayer.

and the Q_z axis is perpendicular to the film plane. The diffraction pattern in Fig. 2 is the intensity distribution along the Q_z axis and the electron-diffraction pattern in Fig. 1(b) is that on the $Q_y - Q_z$ plane. The off-axial measurements are restricted within the reflecting geometry because of strong x-ray absorption by MgO substrate. Then we measured diffracted intensities around 002 and 113 reflections on the $(1\bar{1}0)$ reciprocal-lattice plane, which are shadowed areas in Fig. 3. Figures 4(a) and 4(b) show two-dimensional distributions of diffracted intensities around 002 and 113 reflections for $[\text{Fe}(5 \text{ \AA})/\text{Pt}(13.5 \text{ \AA})]_{15}$ (001) multilayer, respectively. The satellite peaks along the Q_z direction in Figs. 4(a) and 4(b) are due to the modulation of the multilayer perpendicular to the film plane. The spots around (113) show epitaxial relation on the $(1\bar{1}0)$ plane. The Q_z of the fundamental $(113)_0$ reflection satisfies a commensurate relation with that of $(002)_0$ fundamental reflection, namely $Q_z(113)_0 = 1.5 \times Q_z(002)_0$. The relation indicates a fcc structure of the superlattice. The in-plane and out-of-plane epitaxi-

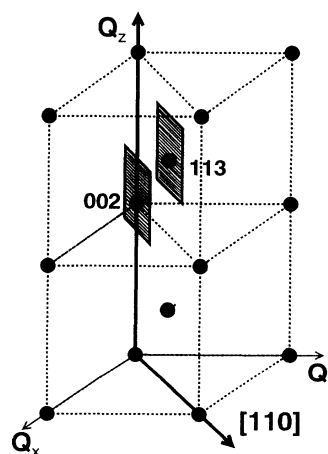


FIG. 3. Schematic diagram of a reciprocal lattice for a fcc lattice. The two-dimensional intensity distributions on the $(1\bar{1}0)$ plane, which is a shadowed area, are measured using a four-circle x-ray diffractometer. The intensity distributions along the Q_z axis are obtained by a conventional x-ray diffractometer. The intensity distributions on the $Q_y - Q_z$ plane are measured by electron diffraction with the electron beam along Ag[100].

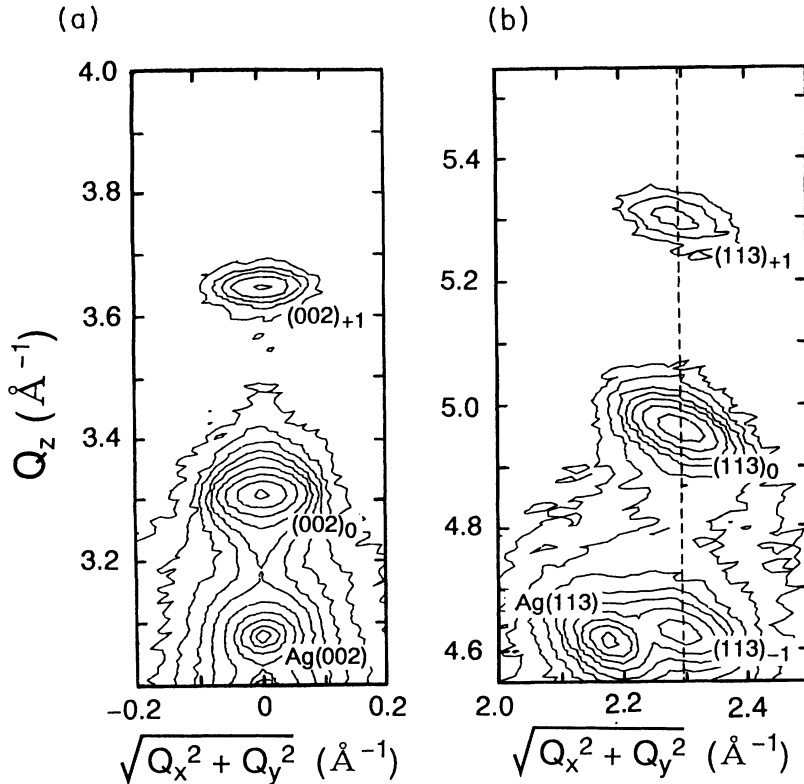


FIG. 4. Q -space logarithmic contour plot of (a) (002) reflections and (b) (113) reflections for a $[\text{Fe}(5 \text{ \AA})/\text{Pt}(13.5 \text{ \AA})]_{15}$ (001) multilayer. The horizontal and vertical axes denote the [110] and [001] directions in the reciprocal-lattice space of fcc Ag, respectively.

al relations by electron diffraction and x-ray measurements suggest that $\text{Fe}(001)\|\text{Pt}(001)$ with a 45° rotation in the plane, so $\text{Fe}[110]\|\text{Pt}[100]$, which agree with results for Fe/Pt(001) multilayer with large modulation length.¹³

The average lattice spacing, $d_{\text{av},\perp}$, which can be calculated by the Q_z of the $(002)_0$ fundamental reflection, should obey the following relation:

$$\frac{\Lambda}{d_{\text{av},\perp}} = \frac{l_{\text{Fe}}}{d_{\text{Fe}}} + \frac{l_{\text{Pt}}}{d_{\text{Pt}}}, \quad (1)$$

where Λ is the period, d_{Fe} and d_{Pt} are the lattice spacings of the Fe and Pt layers, and l_{Fe} and l_{Pt} are the thicknesses of the Fe and Pt layers, respectively.¹⁷ In Fig. 5(a), the average number of atomic planes, $\Lambda/d_{\text{av},\perp}$, is plotted against the Fe layer thickness. The inverse of the slope and the intercept correspond to the lattice spacing of the Fe layer and number of the Pt layer, respectively. The dashed lines in the figure are the calculated ones using the lattice spacings of bulk bcc Fe ($d_{\text{Fe}} = 1.433 \text{ \AA}$) and fcc Fe ($d_{\text{Fe}} = 1.81 \text{ \AA}$). When the Fe layer thickness is relatively large, the lattice spacing approaches that of bulk bcc Fe. For the Fe layer thickness less than 10 \AA , the lattice spacing expands with decreasing Fe layer thickness.

From the (113) peak position on the [110] direction, we can directly calculate the in-plane lattice spacing.¹⁸ Figure 5(b) shows the average (220) lattice spacing, $d_{\text{av},\parallel}$, for Fe/Pt(001) multilayers. The dashed lines represent the (200) lattice spacing of bulk bcc Fe, and the (220) lattice spacings of bulk fcc Pt and fcc Fe. The average lattice spacing obtained by electron diffraction in Fig. 1(b) is

identical to that by off-axial x-ray measurement. For the Fe layer thickness less 8 \AA , the decrease of the average in-plane lattice spacing suggests that the in-plane lattice spacing of the Fe layer is compressed.

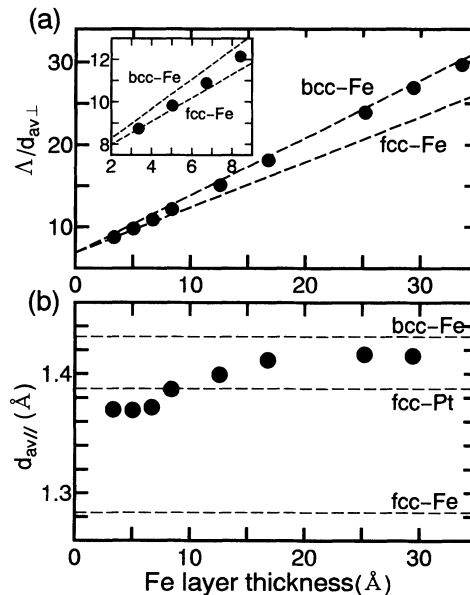


FIG. 5. (a) The average number of lattice plane, $\Lambda/d_{\text{av},\perp}$, for Fe/Pt(001) multilayers with varying the Fe layer thickness. Inset: The average number versus the Fe layer thickness when the Fe layer thickness is small. (b) The average (220) lattice spacing, which is calculated using the $(Q_x^2 + Q_y^2)^{1/2}$ value for the fundamental $(113)_0$ reflections, is plotted against the Fe layer thickness.

We conclude that the Fe layer for epitaxial Fe/Pt(001) multilayer undergoes a phase transition with increasing Fe layer thickness. When the Fe layer thickness is relatively large, the in-plane and out-of-plane lattice spacings are close to those of bcc Fe. With decreasing Fe layer thickness, the in-plane lattice spacing of the Fe layer is compressed and the out-of-plane lattice spacing is expanded. The critical thickness of the Fe layer is around 8 Å. It is small compared with that of an fcc Fe layer grown on Cu(001), which is about 12 ML.⁸

B. Magnetic anisotropy

Magnetic anisotropies per unit area for multilayers are separated into interface and volume contributions:

$$K_{\text{eff}\perp} \times t_{\text{Fe}} = K_{V\perp} \times t_{\text{Fe}} + 2K_{S\perp}, \quad (2a)$$

$$K_{\text{eff}\parallel} \times t_{\text{Fe}} = K_{V\parallel} \times t_{\text{Fe}} + 2K_{S\parallel}, \quad (2b)$$

where $K_{V\perp}$ and $K_{V\parallel}$ describe the volume anisotropies, and $K_{S\perp}$ and $K_{S\parallel}$ the interface anisotropies.^{1,4,19} The subscripts \perp and \parallel represent the directions of the magnetic field. The former is perpendicular the film plane and the latter is parallel to it. Figure 6(a) shows the dependence of the out-of-plane anisotropy per unit area, $K_{\text{eff}\perp} t_{\text{Fe}}$, on the Fe layer thickness. As for epitaxial Fe/Pt(001) multilayers, the slope changes at the Fe layer thickness of 8 Å. On the other hand, the slope for the polycrystalline Fe/Pt multilayer is almost constant. The change corresponds to the lattice deformation as shown in Figs. 5(a) and 5(b). From the linear fits to the data, the volume and interface anisotropies are obtained. They are listed in Table I. The volume anisotropy $K_{V\perp}$ is almost equal for Fe/Pt(001), Fe/Ag(001), and polycrystalline Fe/Pt multilayer, when the Fe layer thickness is larger than 8 Å. On the other hand, $K_{S\perp}$ depends on the nonmagnetic metal and the crystal orientation.

The in-plane anisotropy, $K_{\text{eff}\parallel}$, was measured by a torque magnetometer with the magnetic field parallel to the film plane. Figure 7 is a typical torque curve for a (001) oriented $[\text{Fe}(25.2 \text{ Å})/\text{Pt}(13.5 \text{ Å})]_{15}$ multilayer. The magnetocrystalline anisotropy of a cubic material is expressed as

$$E_a = K_1(\alpha_1^2\alpha_2^2 + \alpha_2^2\alpha_3^2 + \alpha_3^2\alpha_1^2) + K_2\alpha_1^2\alpha_2^2\alpha_3^2, \quad (3)$$

where α_1 , α_2 , and α_3 are direction cosines with respect to the cubic axes. The observed fourfold symmetry is a positive evidence for the in-plane orientation of epitaxially grown Fe layers. The multilayer has an easy axis of mag-

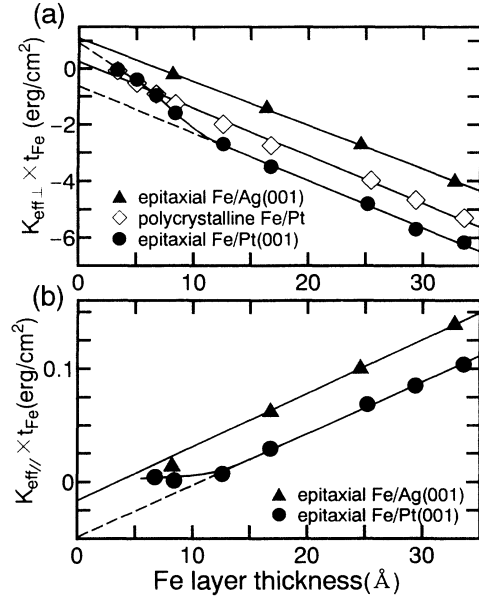


FIG. 6. (a) The out-of-plane and (b) in-plane magnetic anisotropy per unit area for Fe/Pt(001) and Fe/Ag(001) multilayers at room temperature are plotted against the Fe layer thickness.

netization along the [002] direction of bcc Fe and a hard axis along the [022] direction. The difference of amplitude is mainly due to an experimental error. The in-plane magnetic anisotropy per unit area, $K_{\text{eff}\parallel} t_{\text{Fe}}$, is displayed in Fig. 6(b). The fourfold in-plane anisotropy is lost for Fe/Pt(001) multilayers with the Fe layer thickness less than 8 Å. For the Fe layer thickness beyond 10 Å, the in-plane magnetic anisotropy increases linearly. The linear relation suggests that the electronic structure of the interface is independent of the Fe layer thickness. The interface and volume anisotropies are listed in Table I. The volume anisotropy $K_{V\parallel}$ is identical to the magnetocrystalline anisotropy of bulk Fe, which is $4.72 \times 10^5 \text{ erg/cm}^3$.²⁰ There is no magnetoelastic contribution, which is observed for an ultrathin fcc Co(001) film.¹⁹ The in-plane interface anisotropies for Fe/Pt(001) and Fe/Ag(001) multilayers are -0.025 erg/cm^2 and -0.008 erg/cm^2 , respectively. The negative $K_{S\parallel}$ indicates that the magnetocrystalline anisotropy at the interface is different from that of bulk Fe.

C. Magnetization

The saturation magnetization per unit area, $M_S t_{\text{Fe}}$, satisfies the following relation:

TABLE I. The volume and interface anisotropy for the Fe/Pt(001) and Fe/Ag(001) multilayer. The subscript \perp and \parallel represent the magnetic field perpendicular and parallel to the film plane, respectively. The ΔM and M_V are the deviation of the magnetization at the interface and volume magnetization, respectively.

	$K_{S\perp}$ (erg/cm ²)		$K_{V\perp}$ (erg/cm ³)		$K_{S\parallel}$ (erg/cm ²)	$K_{V\parallel}$ (erg/cm ³)	ΔM (emu/cm ²)	M_V (emu/cm ³)
	$t_{\text{Fe}} < 8 \text{ Å}$	$t_{\text{Fe}} > 8 \text{ Å}$	$t_{\text{Fe}} < 8 \text{ Å}$	$t_{\text{Fe}} > 8 \text{ Å}$				
Fe/Pt(001)	0.47	-0.31	-2.8×10^7	-1.7×10^7	-0.025	4.6×10^5	1.6×10^{-5}	1712
Fe/Ag(001)		0.55		-1.6×10^7	-0.008	4.7×10^5	0.2×10^{-5}	1707

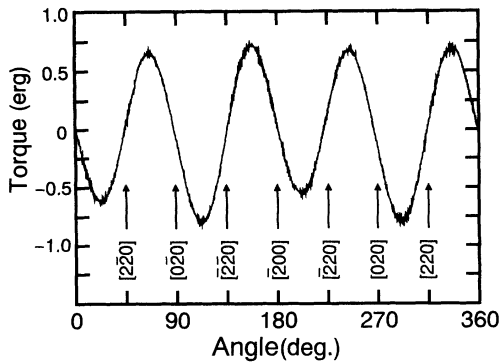


FIG. 7. The torque curve for a $[\text{Fe}(25.2 \text{ \AA})/\text{Pt}(13.5 \text{ \AA})]_{15}$ (001) multilayer measured by a torque magnetometer with the magnetic field parallel to the film plane. The [002] and [022] directions of bcc Fe is shown in the figure.

$$M_s t_{\text{Fe}} = M_V t_{\text{Fe}} + 2\Delta M, \quad (4)$$

where M_V is the volume magnetization and ΔM is the sum of the magnetic contributions from the interface. Figure 8 shows the dependence of saturation magnetization on the Fe layer thickness. The positive intercept for Fe/Pt multilayers shows the existence of a magnetically polarized layer at the interface. The ΔM is independent of the crystal orientation. On the other hand, the ΔM for the Fe/Ag(001) multilayer is small. The M_V for the three systems is almost identical to the quoted value of 1717 emu/cm^3 for bulk bcc Fe. For Fe/Pt(001) and polycrystalline Fe/Pt multilayers with the Fe layer thickness less than 5 \AA , the magnetization decreases compared with that of a bulk bcc Fe. The decrease is not intrinsic but is due to the decrease of Curie temperature. The large change in magnetization due to the structural transition was not observed. This is in contrast with the theoretical result suggesting the drastic decrease of magnetization with the appearance of an fcc structure.²¹

The positive ΔM indicates a magnetostatic contribution to K_{S1} ,² if the polarization decreases exponentially, the contribution is expressed as $\pi M_V \Delta M$, which is 0.086 erg/cm^2 for the Fe/Pt multilayer. Then the net interface anisotropy K_{S1} is -0.23 erg/cm^2 . On the other hand, it is negligible for Fe/Ag multilayers. The volume anisotropy

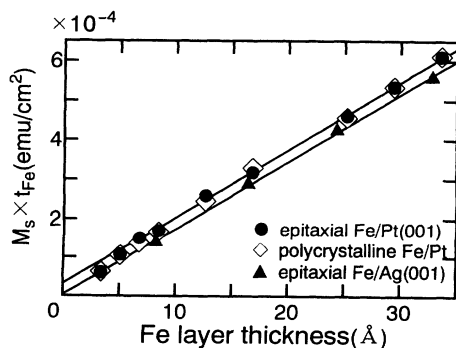


FIG. 8. The saturation magnetization at room temperature versus the Fe layer thickness for Fe/Pt(001), Fe/Ag(001), and polycrystalline Fe/Pt multilayers.

py K_{V1} is almost equal to $-2\pi M_V^2$. This suggests that there is no large magnetocrystalline anisotropy such as an FePt alloy¹³ and that the alloying is relatively small.

Hysteresis loops were measured with the magnetic field applied along the [200] direction, which is the easy axis. In Fig. 9, coercive force is displayed against the Fe layer thickness. The coercive force for the epitaxial Fe/Pt(001) multilayer with the Fe layer thickness less than 8 \AA shows a different behavior compared with those of polycrystalline Fe/Pt multilayers. The difference is due to the structural transition.

D. Interface and volume anisotropy

Leibbrandt, van Wijk, and Habraken have studied the interface structure of Fe(001) with a Pt overlayer by low-energy electron-diffraction experiment.²² It was shown that the alloying occurs at the annealing temperature above 640 K and that the interplanar distance for the first Fe layer is expanded. The inverse photoemission measurement by Himpsel⁶ showed the dependence of an exchange splitting of the Fe layer on the crystal structure. Based on these results, one may expect for the Fe/Pt(001) system that there are little alloying layers at the interface and that the Fe layer at the interface is deformed. It seems that there exists an fcc-like electronic structure at the interface for the Fe/Pt(001) multilayer even when the Fe layer thickness is beyond 10 \AA . The magnetocrystalline anisotropy at the interface is lost and then the $K_{S\parallel}$ is negative. The difference from the bcc electronic structure is more remarkable for Fe/Pt multilayers than for Fe/Ag.

We will investigate the interface and volume anisotropy using a phenomenological model introduced by Néel.²³ The interaction for two atomic magnetic moments is expressed as

$$w(r, \phi) \sim l(r) \left[\cos^2(\phi) - \frac{1}{3} \right] + q(r) \times \left[\cos^4(\phi) - \frac{6}{7} \cos^2(\phi) + \frac{3}{35} \right], \quad (5)$$

where $l(r)$ and $q(r)$ are expansion coefficients, r is the distance between the two atoms, and ϕ is the angle between the direction of the magnetic moment and the line connecting the pair of atoms. Magnetocrystalline anisotropy is obtained from the interaction $w(r, \phi)$ by adding the nearest neighbors.²⁰ Since the coefficient $l(r)$ is usu-

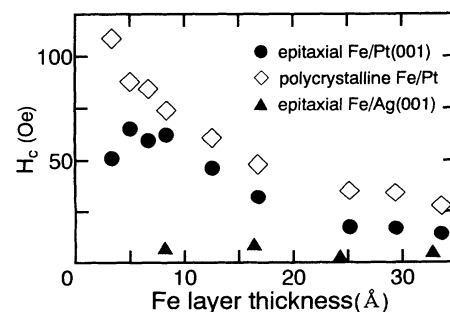


FIG. 9. The coercive force versus the Fe layer thickness for Fe/Pt(001), Fe/Ag(001), and polycrystalline Fe/Pt multilayers.

ally greater than the $q(r)$, the magnetic anisotropy is dominated by the $l(r)$ contribution. The contribution is lost by the cubic symmetry. As for a multilayer, on the other hand, the symmetry is broken by an interface and a strain. The symmetry breaking at the interface gives rise to the $l(r)$ contribution to the $K_{S\perp}$ and the $q(r)$ to the $K_{S\parallel}$. There is no direct correlation between the $K_{S\perp}$ and $K_{S\parallel}$ for (001) oriented films. This is in contrast with results for (110) oriented ones. There exists a relation such as $K_{S\perp} = 2K_{S\parallel}$.¹¹ For Fe/Pt(001) and Fe/Ag(001) multilayers, the observed $K_{S\perp}$ is much greater than the $K_{S\parallel}$. The anisotropy by a uniform strain leads to the $l(r)$ contribution for the $K_{V\perp}$ and the $q(r)$ for the $K_{V\parallel}$. The change of the $K_{V\perp}$ is observed for the Fe/Pt(001) multilayer at the Fe layer thickness of 8 Å. The magnetoelastic calculation² using parameters of a bcc Fe and observed lattice deformation gives a wrong sign. This suggests that the magnetostriction constant λ_{100} for the Fe/Pt(001) multilayer with the Fe layer thickness less than 8 Å should be negative, which is different from that of bcc Fe. The magnetic anisotropy also indicates a structural transition from bcc.

IV. CONCLUSION

The in-plane and out-of-plane epitaxial relations for the Fe/Pt(001) multilayer are shown using off-axial x-ray-

and electron-diffraction measurements. The Fe layer for Fe/Pt(001) multilayer undergoes a structural transition. The critical thickness is around 8 Å. With decreasing Fe layer thickness, the in-plane lattice spacing is compressed and the out-of-plane lattice spacing is expanded comparing with that of bulk bcc Fe. Magnetic anisotropy and coercive force change with the structural transition. When the Fe layer thickness is less than 10 Å, the four-fold in-plane magnetic anisotropy is not observed. The coercive force and out-of-plane magnetic anisotropy $K_{V\perp}$ show a different behavior compared with those of polycrystalline Fe/Pt multilayers. A large decrease of saturation magnetization due to the structural transition was not observed. When the Fe layer thickness is greater than 10 Å, the volume magnetization M_V and in-plane volume anisotropy $K_{V\parallel}$ are identical to those of bulk Fe. The in-plane interface anisotropy $K_{S\parallel}$ is found to be negative.

ACKNOWLEDGMENTS

The author would like to thank Professor T. Shinjo of Kyoto University for helpful discussions and acknowledges Y. Ishikawa of Tosoh Corp. for the TEM measurement, L. Wu of Kyoto University for technical assistance of the x-ray measurement, and Dr. T. Takahata of Tosoh Corp. for useful comments.

- ¹H. J. G. Draaisma, F. J. A. den Broeder, and W. J. M. de Jonge, *J. Magn. Magn. Mater.* **66**, 351 (1987).
- ²M. Sakurai and T. Shinjo, *J. Magn. Magn. Mater.* **128**, 237 (1993).
- ³M. Sakurai and T. Shinjo, *J. Appl. Phys.* **74**, 6840 (1993).
- ⁴P. Krams, F. Lauks, R. L. Stamps, B. Hillebrands, and G. Güntherodt, *Phys. Rev. Lett.* **69**, 3674 (1992).
- ⁵W. Weber, D. A. Wesner, D. Hartmann, and G. Güntherodt, *Phys. Rev. B* **46**, 6199 (1992).
- ⁶F. J. Himpsel, *Phys. Rev. Lett.* **67**, 2363 (1991).
- ⁷G. G. O. Daalderop, P. J. Kelly, and F. H. Schuurmans, *Phys. Rev. B* **42**, 7270 (1990).
- ⁸S. H. Lu, J. Quinn, D. Tian, F. Jona, and P. M. Marcus, *Surf. Sci.* **209**, 364 (1989).
- ⁹R. Allenspach and A. Bischof, *Phys. Rev. Lett.* **69**, 3385 (1992).
- ¹⁰C. Liu, E. R. Moog, and S. P. Bader, *Phys. Rev. Lett.* **60**, 2422 (1988).
- ¹¹H. J. Elmers and U. Gradmann, *Appl. Phys. A* **51**, 255 (1990).
- ¹²K. Shintaku, Y. Daitoh, and T. Shinjo, *Phys. Rev. B* **47**, 14 584 (1993).
- ¹³M. R. Visokay, B. M. Lairson, B. M. Clemens, and R. Sin-

- clair, *J. Magn. Soc. Jpn.* **17**, Suppl. No. S1, 113 (1993).
- ¹⁴B. M. Lairson, M. R. Visokay, R. Sinclair, and B. M. Clemens, *Appl. Phys. Lett.* **62**, 639 (1993).
- ¹⁵P. Etienne, J. Massies, S. Lequien, R. Cabanel, and F. Petroff, *J. Cryst. Growth* **111**, 1003 (1991).
- ¹⁶N. Nakayama, T. Okuyama, and T. Shinjo, *J. Phys. Condens. Matter* **5**, 1173 (1993).
- ¹⁷I. K. Schuller, M. Grimsditch, F. Chambers, G. Devane, H. Vanderstraetan, D. Neerinck, J. P. Locquet, and Y. Bruynseraede, *Phys. Rev. Lett.* **65**, 1235 (1990).
- ¹⁸B. N. Engel, M. H. Wiedmann, R. A. Van Leeuwen, C. M. Falco, L. Wu, N. Nakayama, and T. Shinjo, *Appl. Surf. Sci.* **60/61**, 776 (1992).
- ¹⁹M. Kowalewski, C. M. Schneider, and B. Heinrich, *Phys. Rev. B* **47**, 8748 (1993).
- ²⁰S. Chikazumi, *Physics of Ferromagnetism* (Wiley, New York, 1964).
- ²¹V. L. Moruzzi, *Phys. Rev. Lett.* **57**, 221 (1986).
- ²²G. W. R. Leibbrandt, R. van Wijk, and F. H. P. M. Habraken, *Phys. Rev. B* **47**, 6630 (1993).
- ²³L. Néel, *J. Phys. Rad.* **15**, 376 (1954).

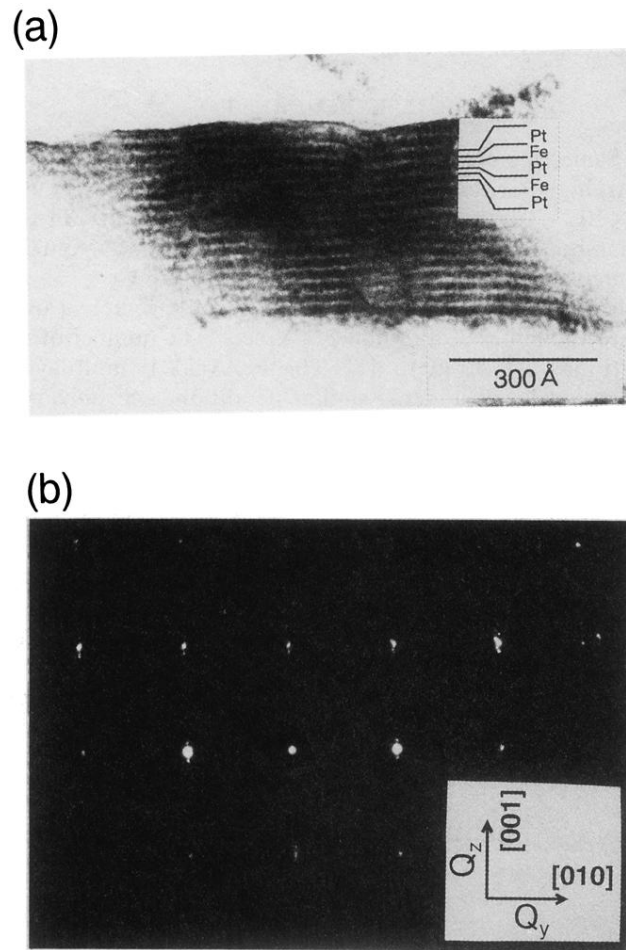


FIG. 1. (a) Cross-sectional TEM image for a $[\text{Fe}(8.4 \text{ \AA})/\text{Pt}(13.5 \text{ \AA})]_{15}(001)$ multilayer. (b) Electron diffraction pattern for the cross sectional specimen, taken with the electron beam along $\text{Ag}[100]$. The satellite peaks along the Q_z direction show the modulation of the multilayer.